In situ observation of the evolution of intragranular acicular ferrite at Mg-containing inclusions in 16Mn Steel

Bin WEN[1),2)] and Bo SONG[1),2)]*

1) State Key Laboratory of Advanced Metallurgy, University of Science and Technology Beijing, Beijing 100083，China

2) Metallurgical and Ecological Engineering School, University of Science and Technology Beijing, Beijing 100083，China

Abstract: The effects of chemical compositions and austenitizing temperature on the formation of intragranular acicular ferrite (IAF) of 16Mn steel, a grade of low alloying steel with carbon content of 0.13~0.19% and manganese content of 1.20~1.60%, were systematically investigated. The in *situ* observation of the evolution of IAF at Mg-containing inclusions was carried out using a high-temperature laser scanning confocal microscopy. The results show that trace amount of Mg can induce the IAF nucleation, while the optimum content of Mg is around 0.0022wt%. The appropriate austenitizing temperature is around 1200℃ and the optimal prior austenite grain size is about 130μm. The temperature range for IAF transformation is around between 571℃ and 627℃, and the time for which is about 12s. The disregistries between Mg-containing inclusions and α-Fe are so small that may act as highly effective nuclei of IAF.

Keywords: magnesium, inclusions, intragranular acicular ferrite, lattice disregistry

1. Introduction

Since the late 1960s, it had been recognized that the inclusions in welding metal could change the microstructures of welding seam [1, 2]. Through the study on the welding microstructures of high strength low alloy steel (HSLA), Harrsion and Farrar [3] had found that the oxides inclusions could induce the formation of intragranular acicular ferrite (IAF) to improve the strength and toughness of welding seam. In the 1990s, the Japanese metallurgical scholars proposed the technical theory of “Oxides Metallurgy” based on the function of oxides inclusions in welding seam, which meaned that during the process of solidification and cooling, the inclusions could be the nucleating cores for sulphides, nitrides, carbides and IAF under certain conditions, so that the grain was refined to improve the toughness and strength of steel [4-7]. Lots of studies have indicated that the inclusions, such as Ti, Al and Zr oxides, Ti, Nb and V carbonitrides, would contribute to the IAF nucleation, and the optimal heterogeneous nucleus was Ti2O3 [8-11]. So far, oxides metallurgy technology has already become an effective way to improve the performance of C-Mn steel, thick plate steel, low carbon non-tempered steel, HSLA and the heat affected zone (HAZ) of weld metal [12].

Generally speaking, the pinning effect of TiN particle is utilized on primary austenite grain (PAG) in the process of welding [13]. However, with the development of large heat input welding technology and increasingly stringent demand for composition control of steels, Ti oxides metallurgy cannot meet this

requirement. On the one hand, part of TiN particles will be redissoluted into the matrix when the heating or welding temperature rises up to 1623K. Owing to lack of suitable heterogeneous nuclei during resolidification, the austenite grain rapidly grow up and the welding performance of steels decrease remarkably [14,15]. On the other hand, the percentage of Ti in some steels is limited, for example, in order to improve the fatigue life of bearing steel, the Ti content must be controlled below 0.005wt%. However, it is too small to play an effective role in inducing the nucleation of IAF. Therefore, it is necessary to find some other elements for oxides metallurgy.

Recently, growing concerns have been focused on the addition of trace Mg into the steel deoxidized by Ti. C.-H.Chang et al. [16] and Han S.Kim et al. [17] who have studied separately the effect of Mg on the variation of inclusions and microstructures during the solidification of steel after deoxidized by Mn-Si-Ti. The results indicated that, with the increasing of Mg, the inclusions were changed as follows: Ti_2O_3(core)+ MnS (periphery)→$MgTiO_3$(core)+MnS(periphery)→MgO(core)+MnS(periphery). Meanwhile, the microstructures of as-cast steels were obviously refined, which contained large numbers of acicular ferrites (AF). Therefore, it could be concluded that trace Mg was good for the heterogeneous nucleation of AF. Through the thermal simulation experiment, CHAI Fen et al. [18] have studied the influences of Mg on the microstructures and impact toughness of the coarse grain heat affected zone(CGHAZ) in the Ti deoxidized steel, and derived that trace Mg (about 0.002wt %) was able to refine the Ti-based inclusions, which resulted in high volume percent of AF in CGHAZ. The Japanese Nippon Steel took advantage of abundant high melting point Mg(O,S), which sizes were as small as 10～100nm, to prevent the growth of the austenitic grain and promote a lot of IAF formation in the process of large heat input welding. So the low-temperature toughness of HAZ was improved significantly [19].

The formation of IAF in steel was influenced by various factors, such as the composition of inclusions, the amount and size of inclusions, the cooling rate, and the parent austenite grain size (PAGS) and so on[20]. Some reports [21,22] pointed out that when the PAGS reached the optimum value, the volume fraction of IAF reached the maximum. For the steel deoxidized by Ti, the relationship between the relative nucleation ability of IAF and PAGS obeyed substantially to C-curve, and it was considered that the best PAGS was among 180-190μm. The study explored by Lee [23] also showed that it contributed to the stable formation of IAF if the PAGS was more than 100μm. Barbaro et al. [21] had found that it could benefit for the IAF precipitation when the PAGS was around 100 μm. Thus, it is concluded that the best PAGS in favor of IAF formation are different for the different types of steels.

In the present paper, using 16Mn steel as a raw material, the effects of chemical compositions, austenitizing temperature and characteristics of inclusions on the nucleation and growth of IAF in 16Mn steel were systematically investigated. The in situ observation of the formation of IAF at Mg-containing inclusions was carried out using a high-temperature laser scanning confocal microscopy (LSCM), which gave direct evidence and kinetic information of IAF. The type of inclusions was clarified by analysis of Factsage software and scanning electron microscope (SEM). Finally, the mechanisms of the formation of IAF were discussed based on the above experiments.

2. Experimental procedure

16Mn steel (6.5kg) was meltted at 1873K in a vacuum induction furnace (100 kHz), which oxygen content is around 120~130 mass ppm. (% and ppm represent mass% and mass ppm, respectively, hereinafter.) After the melting was completed, the initially dissolved oxygen was measured by solid electrolyte oxygen probe, which was around 90ppm. The content of Mg was adjusted by packing the SiMg alloy powders (20wt%Mg and 60wt%Si) on the thin pontil and inserting them into the melt. Then the melt was immediately stirred for 10s using an Al2O3 rod and casted into a pig-iron mold followed by cooling down at an average rate of 3K·s-1. Table 1 shows the chemical composition of prepared samples. The range of Mg content was 0.0013%~0.0054%, which labeled No.2, No.3 and No.4 respectively. For comparison, the original sample was melt with the same method, and which was marked as No.1. Subsequently, the cast ingots were per-forged at 1473K and finish-forged at 1173K to 20 mm diameter bar and then cooled by air cooling. The samples before and after forged were sectioned from the middle with the size of φ10×12mm. They were mechanically ground, polished, prepared as metallographic samples and then subjected to various analyses. The method of quantitative statistics of inclusions in samples was adopted under the 800 times field of view for optical microscope. The morphology and composition of inclusions were examined by scanning electronic microscopy (SEM) equipped with energy dispersive spectrometer (EDS). For observation of the microstructures, the samples were etched for 10-15s using 4% natal, and the average grain size was determined by the linear intercept method.

The in situ observation of microstructure transformation was carried out using a LSCM and an infrared image furnace (IIF). The description of experimental facility was described in detail in the previous research [24, 25]. Fig. 1 shows schematic illustration for the optical system and sample holder in IIF in LSCM system [26]. Due to the acoustic optical deflector, the high scanning rate is as high as 30 frame rate. The samples were machined into disks (7 mm diameter, and 3 mm height), mirror polished, and set into high purity alumina crucible on the platinum holder connected to B type thermocouple. The in situ observation was tested under vacuum condition. The heating cycle is shown in Fig. 2, which consists of three steps: (1) heating up to 1200℃ at a rate of 3.3℃/s, (2) austenitizing at 1200℃ for 600s and (3) continuously cooling to the room temperature with a cooling rate of -5℃/s. The nucleation and growth of ferrites, the formation of IAF induced by inclusions, and the size of austenite grain at 1200℃ was possible to directly observe using this equipment.

Table 1 Chemical compositions of the samples (mass%)

	C	Si	Mn	S	P	Mg	Al	$[O]_{initi.}$	T[O]
No.1	0.12	0.01	0.92	0.01	0.016	---	0.001	0.0092	0.013
No.2	0.12	0.34	0.92	0.01	0.016	0.0013	0.001	0.0087	0.012
No.3	0.12	0.57	0.92	0.01	0.016	0.0022	0.001	0.0092	0.013
No.4	0.12	1.1	0.92	0.01	0.016	0.0054	0.001	0.0093	0.015

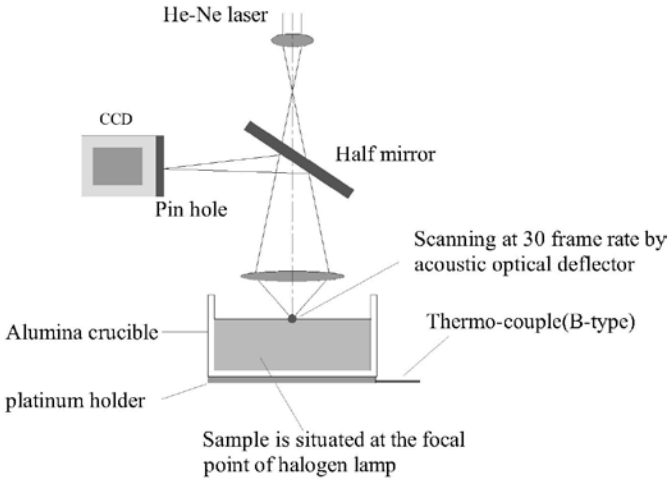

Fig.1. Schematic illustration for the optical system and sample holder in infrared image furnace in LSCM system

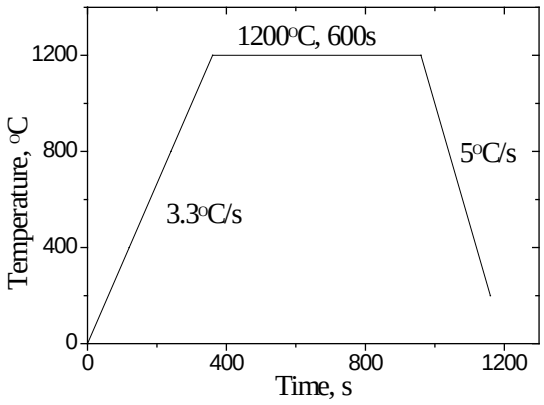

Fig.2. The in *situ* heating cycles set by the IIF-controller system

3 Results and Discussion

3.1 The change of inclusions

FactSage, a thermochemical software with an approach of Gibbs energy minimization [27] was used to perform the thermodynamic calculations in this study. The effects of Mg and O content on the stability of inclusions in 16Mn steel were studied, as shown in Fig. 3. The basic chemical compositions are shown as No.3 in the Table 1, and the contents of Mg and O were chosen from 0 to 0.01wt% and 0 to 0.02wt% respectively. It can be seen that the stable inclusion phases change from MgAl2O4+ Mg2SiO4 to MgO with the increasing of Mg in the melt. However, the precipitation of MgS could take place when Mg reaches 0.0034wt% and while O is lower than 0.0045wt%. Therefore, it is not likely to form MgS in the samples; the dominant inclusions could be MgAl2O4,Mg2SiO4 and MgO in this study.

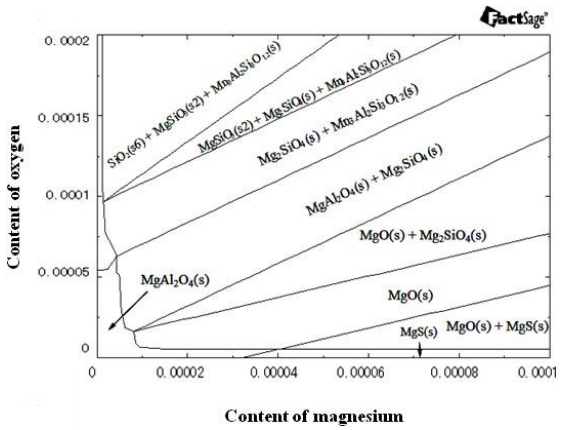

Fig.3 Effects of Mg and O content on the stability of inclusions

The inclusions size distribution of ingots was studied by optical microscope in the view of 800 times, as shown in Fig. 4. It can be seen that most of inclusions in No.1 were larger than 2μm, the percentage of inclusions in sizes 2~5μm was 64.4% and the inclusions less than 2μm was only 10.5%. However, the inclusions were fined obviously after treated by SiMg alloy. In sample No.2 and No.3, the inclusions less than 2μm increased to 71.3% and 82.6%, while the sizes of 2~5μm decreased to 21.8% and 12.8%, respectively. However, owing to appreciably increasing of the number density of inclusions, the collision and aggregation of inclusions would take place when Mg content increased to 0.0054%, so the average size of inclusions in sample No.4 was bigger than that in sample No.2 and No.3.

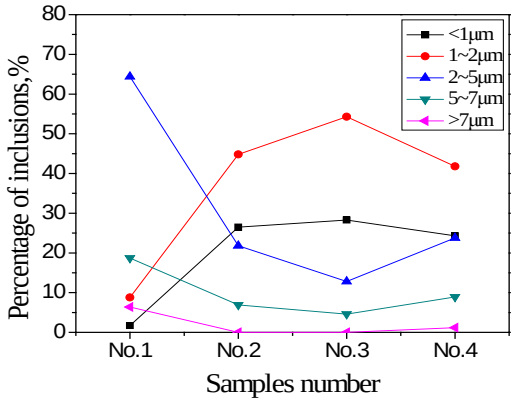

Fig. 4 Inclusions size distribution of No.1~No.4 before forging, No.1, 0%Mg; No.2, 0.0013%Mg; No.3, 0.0022%Mg; No.4, 0.0054%Mg

3.2 Change of microstructures

Microstructures of samples No.1~ No.4 before forging are shown in Fig. 5. The microstructures of No.1 were mainly polygonal ferrite (PF), which nucleated and grew from the austenite grain boundaries. The pearlite (P) was also observed, as shown in Fig. 5(a). In contrast, the microstructures of No.2, No.3 were refined obviously, which consist mainly of interlocking IAF, PF and part of P, as shown in Fig. 5(b) and 5(c). However, the percentage of IAF decreased while the remainder increased in No.4 as shown in Fig. 5(d).

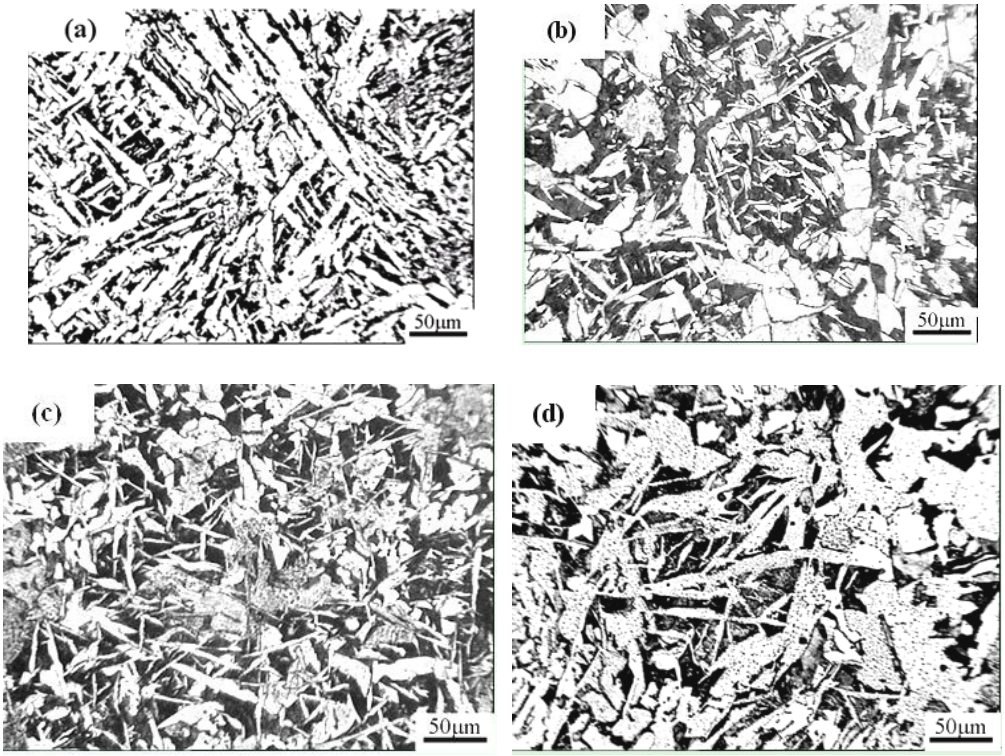

Fig. 5 Microstructures of No.1~No.4 before forging, (a) No.1, 0%Mg; (b) No.2, 0.0013%Mg; (c) No.3, 0.0022%Mg; (d) No.4, 0.0054%Mg

Fig. 6 shows the microstructures of samples after being forged. It can be seen that the microstructures were all refined obviously owing to the effect of forging. The main microstructures of No.1 are block ferrite (BF) and P, and the size of BF was about 20μm, which homogeneously distributed in the entire field of view, as shown in Fig.6(a). It can be seen that the No.2 was refined significantly after adding a small amount of Mg, which consists of BF, IAF and a little of P, as shown in Fig.6(b). When the Mg content in No.3 was increased to 0.0022wt%, a large number of IAF form. Besides, there were a little of intergranular ferrite and P as shown in Fig.6(c). However, the percentage of IAF decreases and BF and P increased when the Mg content in No.4 was increased to 0.0054wt% as shown in Fig.6(d). T. Koseki et al.[28] indicate that IAF development is a result of competition between ferrite nucleation and growth reactions at austenite grain boundary and intragranular inclusion sites. So the inclusion population in steel can dictate the microstructural development. If too few, the formation of IAF is difficult due to the lack of nucleation sites. Whereas too many, owing to collision and growth of inclusions, they will lack the ability to induce the nucleation of IAF, furthermore, which would have great adverse effect on the performance of steel. Therefore, a conclusion can be drawn that trace amounts of Mg in steel can induce the IAF nucleation. With the increasing of Mg, the numerical density of Mg-containing inclusions increases, so the percentage of IAF in steel greatly increases. However, the optimum content of Mg in the steel is about 0.0022wt%.

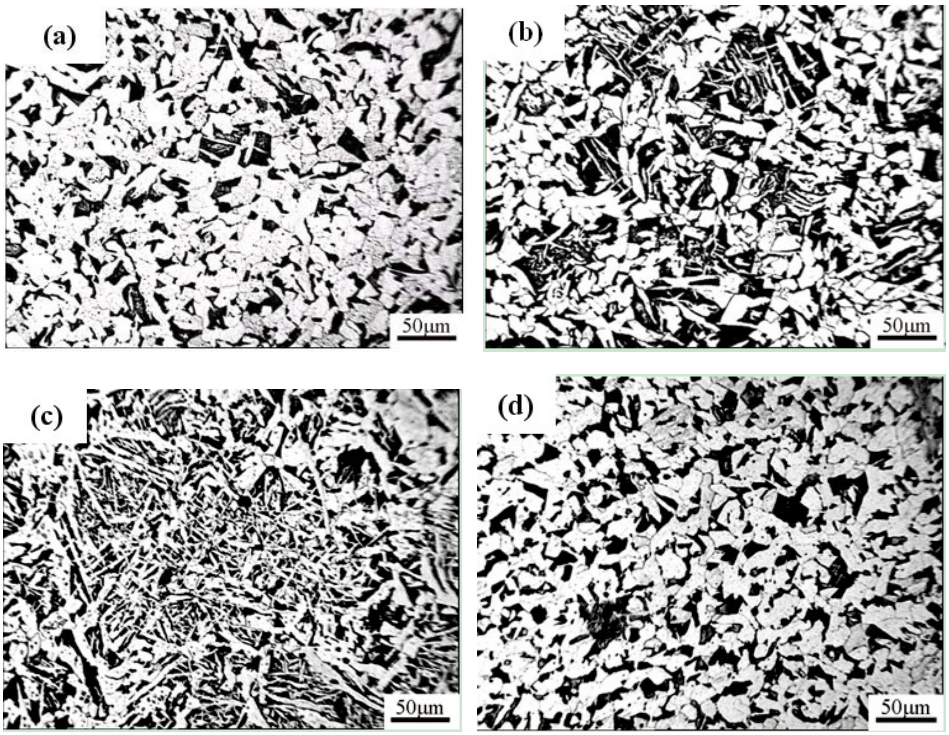

Fig.6 Microstructures of No.1~No.4 after forging, (a) No.1, 0%Mg; (b) No.2, 0.0013%Mg; (c) No.3, 0.0022%Mg; (d) No.4, 0.0054%Mg

3.3 Effect of austenitizing temperature on austenite grain size

The relationship between austenite grain and austenitizing temperature in No.3 was observed by LSCM. The samples were austenitized at 1000, 1100 and 1200℃, and holding for 600s respectively. It can be seen from Fig. 7 that the austenite grains grew rapidly with the increasing austenitizing temperature. The average austenite grain size (AGS) was only about 20μm when the temperature was 1000℃as shown in fig. 7(a). However, when the temperature reached 1100℃, the AGS obviously increased and reached about 100μm as shown in fig. 7(b). The AGS increased to around 130μm with the temperature increase to 1200℃as shown in fig. 7(c). Therefore, for the 16Mn steel treated by Mg, the PAGS which contributes to the formation of IAF is approximately 130 μm, while the optimum austenitizing temperature is 1200℃.

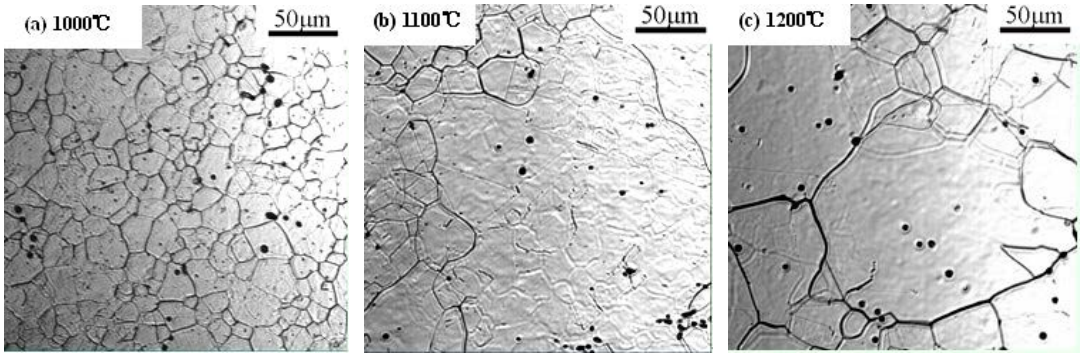

Fig.7 Austenite grains of No.3 at different austenitizing temperature

3.4 In situ observation of phase transformation

Fig.8 shows the results of in situ morphological development of phase transforma- tion for the No.1 austenitized at 1200℃ for 600 s. The inclusions located in the small green circles indicate the nucleation sites of IAFs, and the places within the small red squares show the sites of ferrite grain boundaries. It is interesting to note that there are some lines appear near the inclusions when the temperature droped to 705℃ in Fig. 8(a). However, since they were observed above 1000 ℃, they can be e high temperature. When the temperature droped to 664℃, a little of ferrite precipitated and grew on AGBs and inclusions in the grains, as shown in Fig. 8(b). With the temperature decreasing, it can be seen that GBFs and IAFs nucleated and grew up rapidly based on the AGBs and inclusions respectively. Many studies[29-32] indicate that the size of inclusions as the nucleus of IAF are about 1μm. While the inclusions in No.1 were more large, their sizes were around 5μm, so the number of inclusions acting as nucleus was fewer as shown in Fig.8(c), (d) and (e). When the temperature droped to 586℃, part of secondary ferrites were induced by the primary ferrite phase as shown in Fig.8(f). When the temperature droped to 579℃, the transformation process of GBF and IAF was almost over as shown in Fig.8(g). Fig.8(h) is the microstructure of the other field of view. It can be seen that the nucleation inclusions were so few that the percentage of IAF was small.

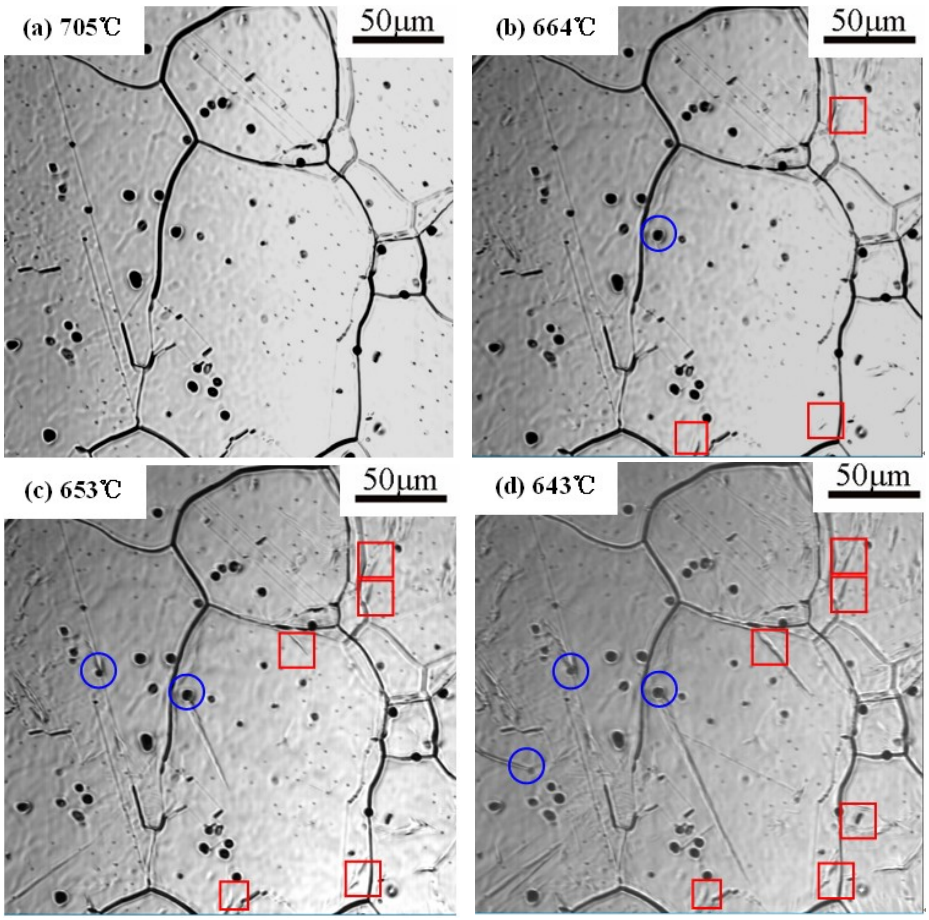

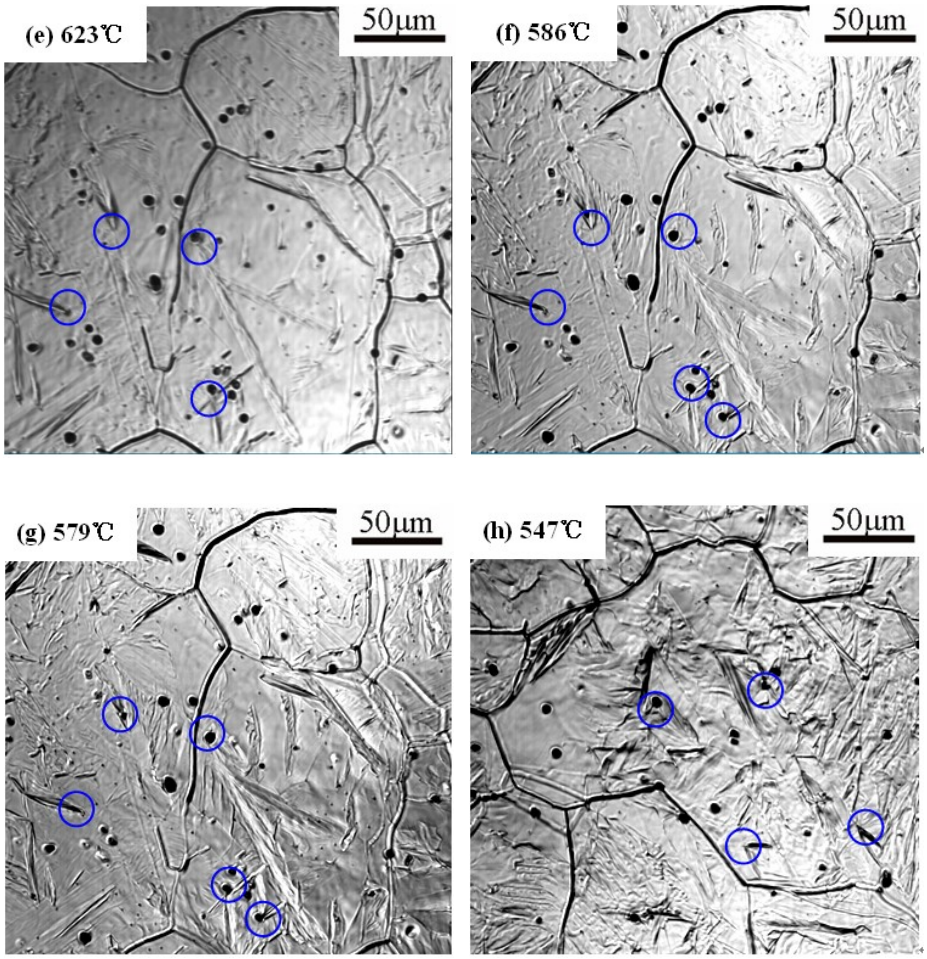

Fig.8. In situ morphological development of phase transformation for the sample No.1 austenitized at 1200℃ for 600 s

Fig.9 shows the results of in situ morphological development of phase transforma -tion for the No.3 austenitized at 1200 ℃ for 600 s. When the temperature dropped to 654℃, a little of ferrite would precipitate at AGBs, which is indicated by red small blocks in Fig. 6(b). On the one hand, the cause could be that the energy barrier near the AGBs was lower than intragranular inclusions. On the other hand, the diffusion rates of chemical elements at AGBs were faster. So it can be concluded that AGBs could be the preferential nucleation sites of ferrite during the transformation of the undercooled austenite. However, a little of IAF may begin to nucleate and grow at intragranular inclusions as the small blue circle shown in Fig. 6(c), meanwhile, the amount of GBF increased significantly. The IAF dramatically increased and the GBF further grew with the decrease of temperature, as shown in Fig. 6(d). In conclusion, the nucleation process may be dominated by the effect of AGBs at the beginning of transformation. The IAF nucleation was then likely to be controlled by the inclusions as the transformation proceeded. Fig. 6(e), (f) and (g) show that most of the IGFs precipitate at the inclusions, at the same time, part of secondary ferrites were induced by the primary ferrite phase. When the temperature dropped to 528℃, the processes of GBF and IAF evolution almost finished as shown in Fig. 6(h). From the above analysis it can be drawn, the temperature range for IAFs transformation was around 571 ℃~627℃, and

the IAF nucleation and growth completed within a short time, which was about 12s. It is consistent with the results of the investigation in Reference [29].

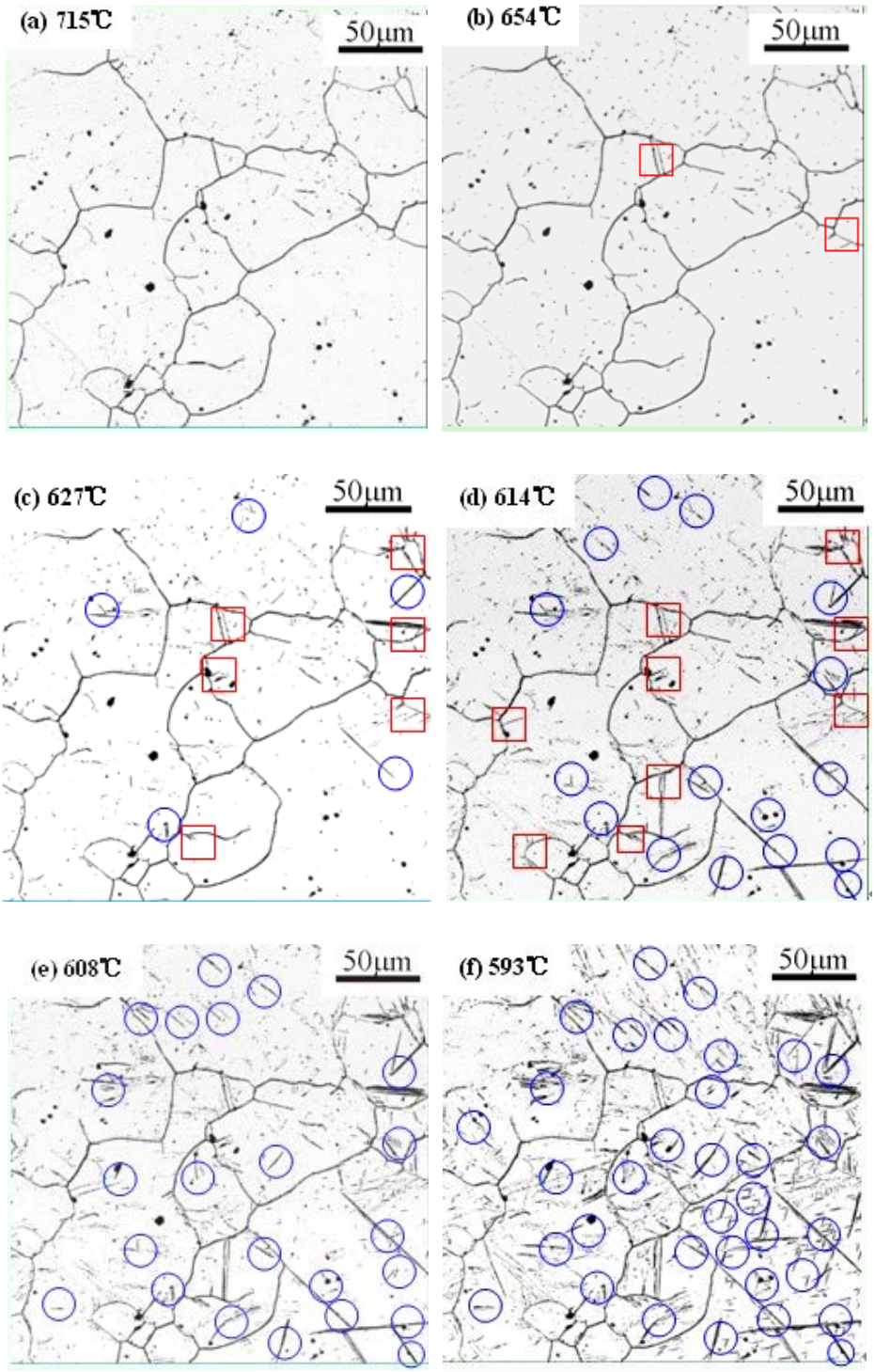

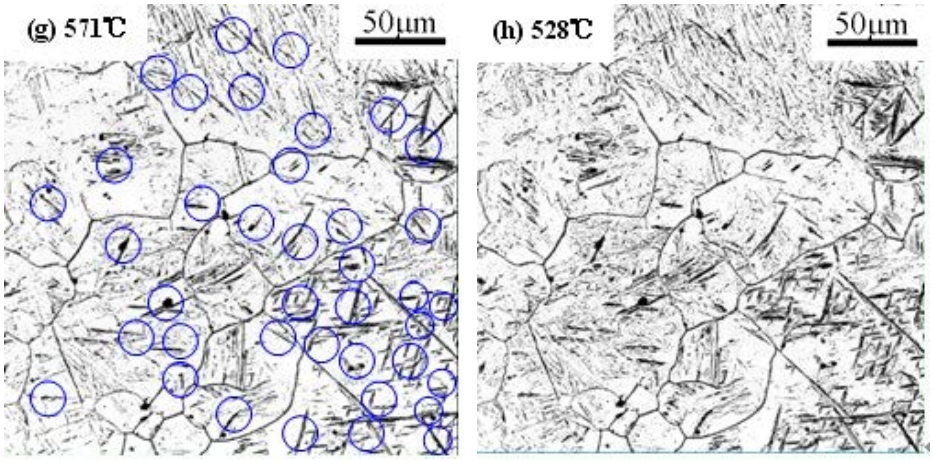

Fig.9. In situ observation of morphological development of phase transformation for the No.3 austenitized at 1200 ℃ for 600 s

The IAF nucleation on inclusions in No.3 was analysed by SEM and EDX as shown in Fig. 10. There were around three primary IAF lathes nucleated on the inclusions, indicated by black arrow in Fig. 10(a). The size was about 1~2μm and the composition mineral phases were MgAl2O4 and Mg2SiO4 from the analysis of EDS, as shown in Fig. 10(b).

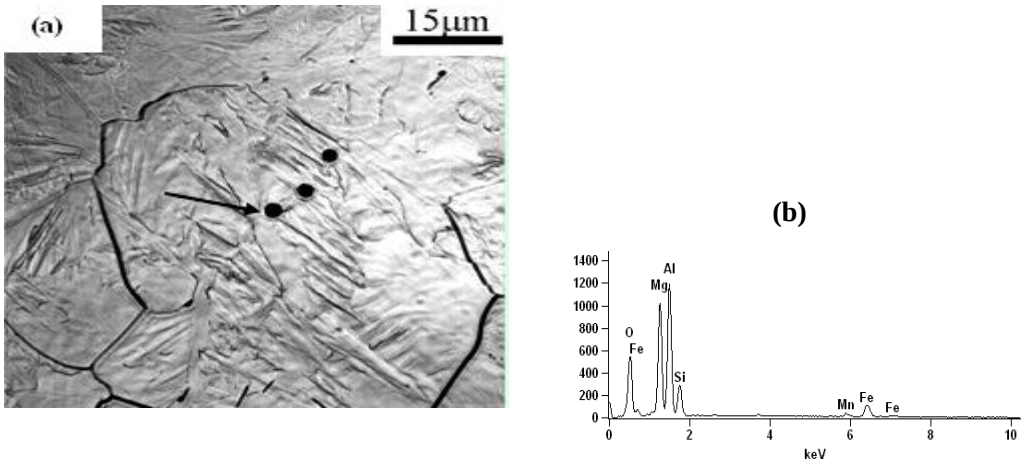

Fig.10. SEM and EDX analyses of IAF nucleation on inclusions in No.3, (a) SEM, (b) EDX

Fig. 11 shows the results of in situ morphological development of phase transfor- mation for the No.3 austenitized at 1000 ℃ for 600 s. It can be seen that lots of BF form on the AGBs with temperature decreasing. By comparison with the situation of austenitizing at 1200℃, the austenitizing temperature was so low that the austenite grains were very small, and it led to significant increase of the nucleation sites of GBF. Therefore, the nucleation and growth of ferrites were almost at AGB and a few inclusions can play the role in inducing IAF nucleation, as shown in Fig. 10(c), (d), (e) and (f).

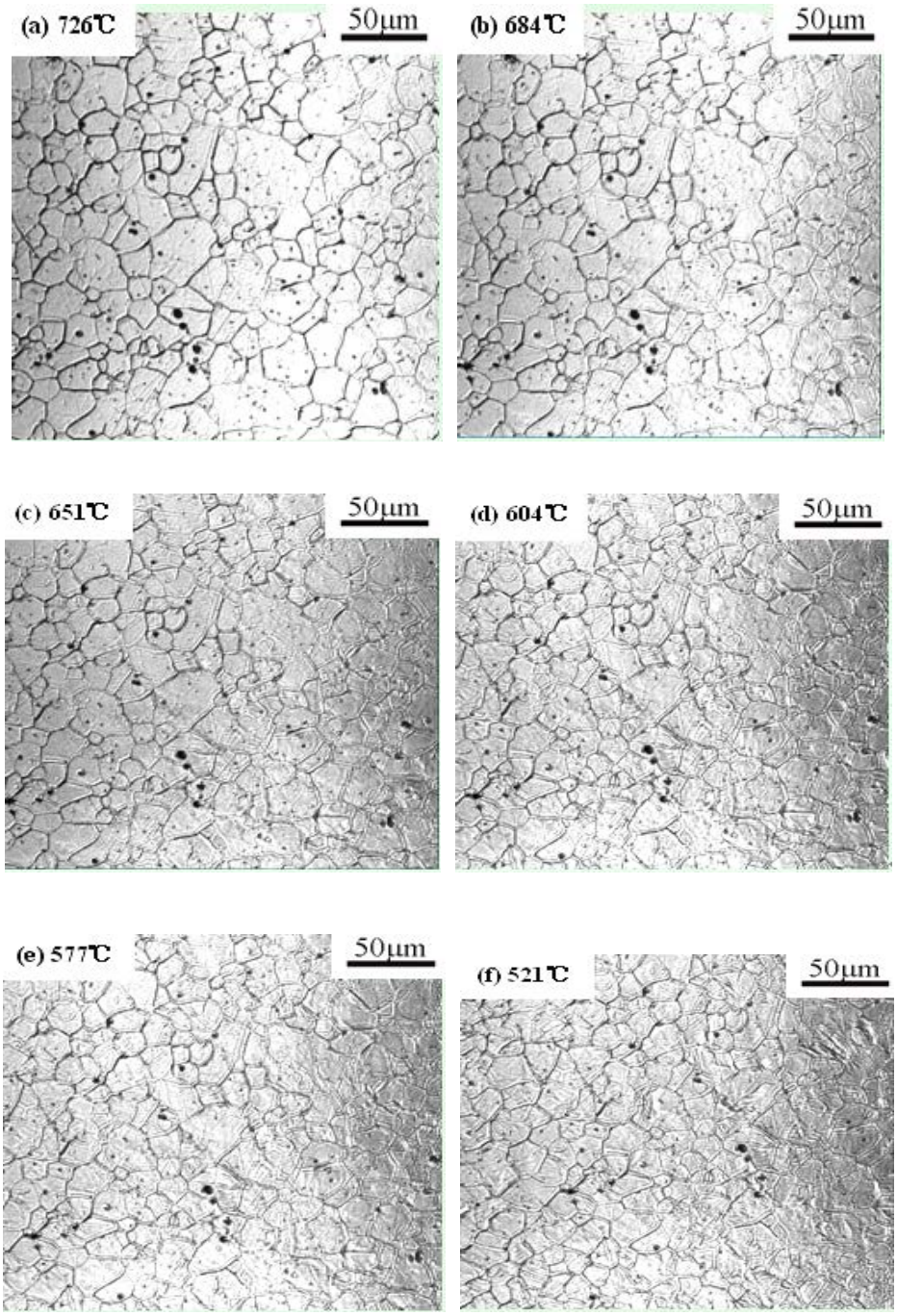

Fig.11 In situ observation of morphological development of phase transformation for the No.3 austenitized at 1000℃ for 600 s

3.5 Mechanism of nucleation

So far, a number of different mechanisms have been proposed to explain the function of non-metallic inclusions on the nucleation of IGF: (1) Increasing stress fields around the inclusions resulted from the differences in thermal expansion coefficients between austenite matrix and inclusions[34]; (2) There is a small

lattice disregistry between inclusions and ferrite, so the energy of nucleation of IGF on the inclusions is quite low to make it easier that IGF precipitates and grows[35]; (3) Inclusions can absorb Mn nearby the austenite to form the Mn-depleted zone and lower the stability of austenite, which inducing the IGF nucleation and growth on inclusions[36-38]; (4) Offering an inert surface that can reduce the nucleation free energy barrier for the ferrite embryo localized variations in chemical composition around inclusions[39]. Of these, (2) and (3) have the most persuasive suggestion.

According to the heterogeneous nucleation theory proposed by Turnbull[40], the disregistry between some low-index planes of inclusion and metal phase can be very small. The smaller the disregistry is, the lower the interfacial energy required for the transformation is, so it is easier for the nucleation of inclusion phase to take place and the grain size of crystallization becomes smaller. The two-dimensional model proposed by Bramfitt [35] is applied to calculate the lattice disregistry between inclusions and α-Fe phase, as shown by the Eq.(1).

$$\delta_{(hkl)_n}^{(hkl)_s} = \sum_{i=1}^{3} \frac{\left| (d_{[uvw]_s^i} \cos\theta) - d_{[uvw]_n^i} \right|}{\frac{d_{[uvw]_n^i}}{3}} \times 100\% \quad (1)$$

where $(hkl)_s$ is a low-index plane of the nucleus, $[uvw]_s$ a low-index direction of $(hkl)_s$, $(hkl)_n$ is a low-index plane of the nucleated phase, $[uvw]_n$ a low index direction of $(hkl)_n$, d the interatomic spacing, and θ the angle between $[uvw]_s$ and $[uvw]_n$.

It suggests that, when the disregistry is smaller than 6.0, the inclusion is extremely effective in inducing the IAF nucleation. If the value is between 6.0 and 12.0, it is moderately effective for the nucleation. However, if the value is greater than 12.0, it has no effect on the nucleation of IAF.

The disregistries between Mg-containing inclusions and α-Fe phase were calculated at 1185K (γ→α start temperature) and listed in the Table 2. The disregistries between MgAl2O4, MgO and α-Fe are as small as 0.6% and 4.03% respectively. Therefore, they can act as highly effective nuclei of α-Fe phase during γ→α transformation and facilitate the nucleation of IAF.

Table 2 Lattice disregistry between Mg-containing inclusions and α-Fe at 1185 K

Inclusion	Lattice structure	Lattice parameter, a / nm	$a/a_{\alpha\text{-Fe}}$	Disregistry
$MgAl_2O_4$	Cubic	0.8155	2.845	0.6%
MgO	Cubic	0.4268	1.489	4.03%
MgS	Cubic	0.5272	1.839	9.14%

4. Conclusions

The effects of chemical compositions and austenitizing temperature on the formation of intragranular acicular ferrite (IAF) of 16Mn steel were systematically investigated by in situ observation of the evolution of IAF at Mg-containing inclusions using a high-temperature laser scanning confocal microscopy. The following conclusions can be drawn.

(1) Mg has a great effect on the inclusions and microstructures of 16Mn steel. The inclusions in 16Mn steel treated by Mg can be transformed into $MgAl_2O_4$, Mg_2SiO_4 and MgO. Trace amount of Mg can induce the IAF nucleation. With the increasing of Mg addition, the percentage of IAF in steel greatly increases. However, the optimum content of Mg in 16Mn steel is around 0.0022wt%.

(2) Austenitizing temperature has a great influence upon the microstructure and PAGS of the 16Mn steel treated by Mg. The optimum austenitizing temperature is about 1200℃ and the PAGS is around 130 μm in favour of the formation of IAF.

(3) The temperature range for IAF transformation is around 571 ℃ 627℃, and the IAF nucleation and growth complete within a short time, which is about 12s.

(4) The disregistries between $MgAl_2O_4$, MgO and α-Fe are as small as 0.6% and 4.03%. It may act as highly effective nuclei of α-Fe phase during γ→α transformation and facilitate the nucleation of IAF.

Acknowledgements

The authors are grateful to the support of National Natural Science Foundations of China (NSFC) (No. 50734008) and the Fundamental Research Funds for the Central Universities (No. FRF-MP-09-001A). The authors also appreciate the assistance with the experiments from PhD Jiang Min and PhD candidate Hu Zhiyong at University of Science and Technology Beijing (USTB).

References

[1] K, Gloor: *IIWDOC II-A-106-63*, (1963).
[2] K. Katoh: *IIW DOC II-A-158-65*, (1965).
[3] P. L. Harrison and R. A. Farrar: *J. materials sci.*, 16(1981), 2218.
[4] J. Takamura and S. Mizoguchi: Proceedings of the sixth international iron and steel congress, Nagoya, *ISIJ Int.*, (1990), 591.
[5] S. Mizoguchi: Proc.6th. Inter. Iron & Steel Cong., Nagoya, *ISIJ Int.*, (1990), 598.
[6] T. Sawai: Proc.6th. Inter. Iron & Steel Cong., Nagoya, *ISIJ Int.*, (1990), 605.
[7] S. Ogibayashi: Proc.6th. Inter. Iron & Steel Cong., Nagoya, *ISIJ Int.*, (1990), 612.
[8] A. M. Guo, S. R. Li, J. Guo, et al.: Mater. Char., 59(2008), 134.
[9] G. Øystein , K. Leiv , E. Casper: *ISIJ Int.* 46(2006), 824.
[10] S. S. Babu, S. A. David: *ISIJ Int.* 42(2002), 1344.

[11] S. Talas, R.C. Cochrane: *Journal of Alloys and Compounds*, 396(2005), 224.
[12] Z. Z. Liu, M. Kuwabara: *Steelmaking*, 23(2007), 1.
[13] M. Minagawa, K. Ishida, Y. Funatsu, Nippon Steel Tech. Rep. 380 (2004) 6-8.
[14] M. Nagahara, H. Fukami, Nippon Steel Tech. Rep. 380 (2004) 9-11.
[15] K. Akihiko, Y. Ken-Ichi, H. Tomohiko, et al., Nippon Steel Tech. Rep. 380 (2004) 39-44.
[16] C.-H.Chang, I.-H.Jung, S.-C.Park,et al, Ironmaking and Steelmaking 32(3) (2005) 251-257.
[17] S.K. Han, C.H. Chang, H.G. Lee, Scripta Materialia 53 (2005) 1253–1258.
[18] F. Chai, C.F. Yang, H. Su, et al., jour. of iron and steel research int.16(1) (2009) 69-74.
[19] Akihiko KOJIMA, Akihito KIYOSE, Ryuji UEMORI et al., Nippon Steel Tech. Rep. 380 (2004) 2-5.
[20] C.W. Bale, P. Chartrand, S.A. Degterov, et al., Calphad 26(2) (2002) 189-192.
[21] Z. Y. Zhang, R. A. Farrar, Mater. Sci Technol., 12(3) (1996) 260-266.
[22] S. C. Han, Dev Appl Mater., 10 (5) (1995) 2-7.
[23] T. Koseki, G. Thewlis, Mater. Sci. Technol., 21(8) (2005) 867-879.
[24] Y. Komizo, H. Terasaki, M.Yonemura: Welding in the World, 52 (2008), No.5, 56.
[25] H. Yin, H. Shibata, T. Emi, M. Suzuki: ISIJ International, 37(1997), No.10, 936.
[26] H. Terasaki and Y. Komizo: Science and Technology of Welding and Joining, 11 (2006), No.5, 561.
[27] C.W. Bale, P. Chartrand, S.A. Degterov, et al.: *Calphad*, 26(2002), 189.
[28]. T. Koseki and G. Thewlis: *Mater. Sci. Technol.*, 21 (2005), 867.
[29] T. K. Lee, H. J. Kim, B. Y. Kang, S. K. Hwang:*ISIJ Int.*, 40(2000), 1260.
[30] D. S. Sarma, A. V. Karasev, P. G. Jonsson: *ISIJ Int.*, 49(2009), 1063.
[31] A. Hajeri, F. Khaled: *ISIJ Int*., 46(2006), 1233.
[32] J.-L. Lee: *Acta Metallurgica et Materialia*, 42(1994), 3291.
[33] D. Zhang, H. Terasaki, Y. Komizo: *Acta Materialia*, 58(2010), 1369.
[34] G. S. Barritte, D.V. Edmonds: *The Met. Soc.*, London, (1981), 126.
[35] B. L. Bramfitt: *Metal. Trans.*, 7 (1970), 1987.
[36] K. Yamamoto, T. Hasegawa, J. Takamura: *ISIJ Int.*, 36(1996), 80.
[37] H. Mabuchi, R. Uemopi, M. Fujioka: *ISIJ Int.*, 36(1996), 1406.
[38] G. Shigesato, M.Sugiyama, S. Aihara, et al.: *Tetsu-to-Hagane*, 87(2001), 93.
[39] Z. Zhang, R.A. Farrar: *Mater. Sci. Technol.* 12 (1996), 237.
[40] D. Turnbull, B. Vonnegut: *Industrial and Engineering Chemistry*, 44(1952), 1292.